VST

PRELIMINARY DESIGN REVIEW

SECTION 2

OPTICAL DESIGN

Designed by :	**D. Mancini, D. Ferruzzi, G.Marra,**
Signature	
FEA by :	**D. Mancini, F. Perrotta**
Signature	
SW tools by :	**M. Brescia**
Signature	
Prepared by :	**D.Ferruzzi, G.Marra**
Signature	
Supervised by :	**D. Mancini, G.Sedmak**
Signature	
Verified by :	**D. Mancini, G. Sedmak, V. Fiume Garelli**
Signature	
Approved by :	**G. Sedmak**
Signature	

EVOLUTION RECORD

Issue	Revision	Date	Notes
1.0	0	15/11/98	First release for comments
2.0	0	18/12/98	Added focus depth and FEA interface analysis
2.1	1	22/12/98	Some errors removed

TABLE OF CONTENTS

2 Telescope Optical Design 5

2.1 Introduction 5
2.2 Optical design requirements 5
2.3 Optical layout 6
2.3.1 Shack Hartmann optical subsystem 10
2.4 Optical performance 10
2.4.1 Encircled Energy 10
2.4.2 Spot diagram 12
2.4.2.1 Spot diagram with interference filters 13
2.4.3 MTF 14
2.4.4 Field curvature and distortion curves 15
2.4.5 Analysis of focus depth 17
2.5 Efficiency curves for the two configurations 18
2.5.1 Efficiency with ADC and one lens field corrector 18
2.5.2 Efficiency with two lenses field corrector 19
2.6 Ghost Analysis 20
2.6.1 Ghost analysis with ADC and one lens field corrector 20
2.6.2 Ghost analysis with two lenses field corrector 23
2.6.3 Analysis of focused ghosts 25
2.6.4 Analysis of sky concentration 25
2.6.5 Ghost analysis summary 25
2.7 Optical tolerances 26
2.8 First stage of baffles design 29
2.9 Image quality versus mirror deformation 30
2.9.1 Image quality versus mirror deformation for two lenses corrector 31
2.9.2 Image quality versus mirror deformation for ADC and one lens corrector 33

TABLE & FIGURES INDEX

Tab. 2.1 - Main requirements for the optical design 5
Tab. 2.2 - VST main optical data 8
Tab. 2.3 - VST mirrors optical data 9
Tab. 2.4 - VST optical data for ADC and one lens, in, B, V, R, I bands 9
Tab. 2.5 - VST optical data for two lenses corrector, filter and dewar window in U ÷ I bands 9
Tab. 2.6 - Optical performance for the configuration with two lenses 10
Tab. 2.7 - Optical performance for the configuration with the ADC and one lens 10
Tab. 2.8 - Depth of focus versus EE % variation for the configuration with the ADC and one lens at 70°zenith angle 17
Tab. 2.9 - Depth of focus versus EE % variation for the configuration with the ADC and one lens at 0°zenith angle 17
Tab. 2.10 - Depth of focus versus EE % variation for the configuration with the two lenses at zenith 17
Tab. 2.11 - Table of all possible ghosts for ADC and one lens corrector configuration 22
Tab. 2.12 - Table of all possible ghosts for two lenses corrector configuration 24
Tab. 2.13 - Summary of the brightest focused ghosts 25
Tab. 2.14 - Summary of most focalised ghost for sky concentration 25
Tab. 2.15 - Centred tolerances for two lenses field corrector 26

Tab. 2.16 - Centred tolerances for one lens field corrector and ADC 26
Tab. 2.17 - Decentred tolerances for two lenses field corrector....................27
Tab. 2.18 - Decentred tolerances for one lens field corrector and ADC 27
Tab. 2.19 - Performance of polychromatic MTF for two lenses field corrector (320 ÷ 1014nm) at z=0....................28
Tab. 2.20 - Performance of polychromatic MTF for ADC and one lens corrector (365 ÷ 1014nm) at z=0 28

Fig. 2.1 - VST complete optical layout of telescope with one lens and the ADC, with a curve dewar window...........6
Fig. 2.2 - VST zoom of the optical layout of the corrector with one lens and the ADC, with a curve dewar window..6
Fig.2.3 - VST optical layout of telescope with two lenses (U ÷ I bands)....................7
Fig.2.4 - VST zoom of the optical layout of the two lenses (U ÷ I bands)....................7
Fig.2.5 - Encircled Energy for two lenses field corrector at zenith 11
Fig.2.6 - Encircled Energy for ADC and one lens corrector at 0°zenith distance 11
Fig.2.7 - Encircled Energy for ADC and one lens corrector at 70°zenith distance 12
Fig.2.8 - Spot diagram for one lens and ADC at zenith from B to I 12
Fig.2.9 - Spot diagrams for one lens and ADC at z=70°zenith distance....................13
Fig.2.10 - Spot diagram for two lenses corrector from U to I bands at zenith....................13
Fig.2.11 - MTF two lenses field corrector at zenith 14
Fig.2.12 - MTF ADC an one lens corrector at 0°zenith distance 14
Fig.2.13 - MTF ADC an one lens corrector at 70°zenith distance 15
Fig.2.14 - Field curvature and distortion curves for the configuration with one lens and ADC at z angle of 70°zenith distance....................16
Fig.2.15 - Field curvature and distortion curves for the configuration with two lenses....................16
Fig.2.16 - Efficiency curves for ADC and one lens corrector at z=0....................18
Fig.2.17 - Efficiency curves for two lenses corrector....................19
Fig.2.18 - ADC and one lens 20
Fig.2.19 - Two lenses corrector....................23
Fig.2.20 - First stage of baffle design....................29
Fig.2.21 - OAC Telescope optical quality optimisation work flow....................30
Fig.2.22 - Encircled Energy for two lenses field corrector at zenith with M1 gravitational loads applied....................31
Fig.2.23 - Spot diagram with two lenses corrector at zenith with M1 gravitational loads applied....................32
Fig.2.24 - Field curvature and distortion curves for the configuration with two lenses at zenith with M1 gravitational loads applied....................32
Fig.2.25 - Encircled Energy for two lenses field corrector at zenith with M1 gravitational loads applied....................33
Fig.2.26 - Spot diagram for one lens and ADC at zenith with M1 gravitational loads applied....................34
Fig.2.27 - Field curvature and distortion curves for the configuration with one lens and ADC at 0°zenith angle with M1 gravitational loads applied....................34

2 TELESCOPE OPTICAL DESIGN

2.1 INTRODUCTION

In this document, a new optical solution for the VST is reported. As in the baseline of 06/11/98 it has a removable ADC and a curve dewar window, the clear aperture diameter is 2610 mm. It is provided with a corrector made of two lenses from U to I bands (0.320 ÷1.014 μm) and a corrector with one different lens and an ADC with curve entrance and exit surfaces from V to I bands (0.365 ÷ 1.014 μm). The ADC type chosen is constituted of two couples of prisms, which glasses were substituted with PSK3 and LLF1, because the latter, respect to BK7 and LLF6 have the same index of refraction at one wavelength (441.8 nm). In this way the positions of the centroid of spot don't change significantly when observing at different angles. The two double prisms must be suitably counter rotated, to correct the atmospherical dispersion at the different observation angles, respect to zenith. The results of the study of optical quality were reported at zenith angle and at the z angle corresponding to the maximum dispersion of ADC. The parameters of the mirrors were unchanged, with respect to the baseline of 06/11/98, while those of the two correctors, filter and dewar window were re-optimised. In particular the thickness of dewar window was increased, so the distance between M1 and the focal plane. The change of glasses for ADC let to increase the equivalent focal length of the telescope when re-optimising the two correctors. So, respect to the baseline of 06/11/98 it was possible to normalise not only the curvatures of the ADC and one lens corrector, but also all those of the two lenses corrector, still obtaining a good optical quality for both configurations. In particular, the solution found for two lenses corrector shows an optical quality which is close to the goal. It represents a compromise between the maximum achievable distance of last corrector element from the dewar window, and the maximum acceptable percent distortion. If the distance between last lens of the corrector with two lenses is further increased, percent distortion rises critically.

2.2 OPTICAL DESIGN REQUIREMENTS

Table 2.1 summarises the top-level requirements for the nominal design of the telescope optics as well as the dimensional requirements. The additive constraint, coming from the mechanics of the camera on the minimum distance between last corrector element and dewar window was also considered.

Telescope diameter	2610 mm		
Image Scale	0.21 arcsec/pixel		
Pixel size	15 μm		
Unvignetted field of view	1.47° diagonal		
Image quality	Required	80% energy within 2 × 2 pixels	
	Goal	80% energy within 1 × 1 pixel	
Maximum distortion	Required	≤ 0.3%	
	Goal	≤ 0.01%	
Wavelength range	Without ADC	0.320 to 1.014 microns	
	With ADC	0.365 to 1.014 microns	
Zenithal distance range	Min. 0-60°		
Max. backfocal distance M1 vertex to focus			1500 mm
Min. distance M1 vertex to first optical surface			400 mm
Max. footprint diameter of light beams in M1 center hole			500 mm
Min. backfocal distance last corrector element to image surface			200 mm
Min. backfocal distance last corrector element to dewar window			245 mm
Min. distance back surface of dewar window to image surface			22.00 mm
Minimum thickness of dewar window			20.0 mm

Tab. 2.1 - Main requirements for the optical design

2.3 OPTICAL LAYOUT

The mirrors parameters are the same of the solutions of 31/07/98 and of 06/11/98, while those of the two correctors and dewar window were modified. As in the solution of November, the last corrector element was moved away from the dewar window in order to have much more space for the mechanics of the camera. The thickness of dewar window was instead modified and increased for safety and the ADC glasses were changed from UBK7 and LLF6 to PSK3 and LLF1 which have the same index of refraction at one wavelength, so the centroid of spot doesn't move substantially at different observing angles. All correctors and dewar window parameters were re-optimised. With the change of the glasses of ADC, it was possible to increase the back focal length in order to meet optical quality requirements, also with all two lenses corrector surfaces normalised to DIN tables, keeping percent distortion low. In Fig. 2-1 and 2-2, the complete optical layout of the telescope with one lens and the ADC and the zoom of the corrector are respectively shown.

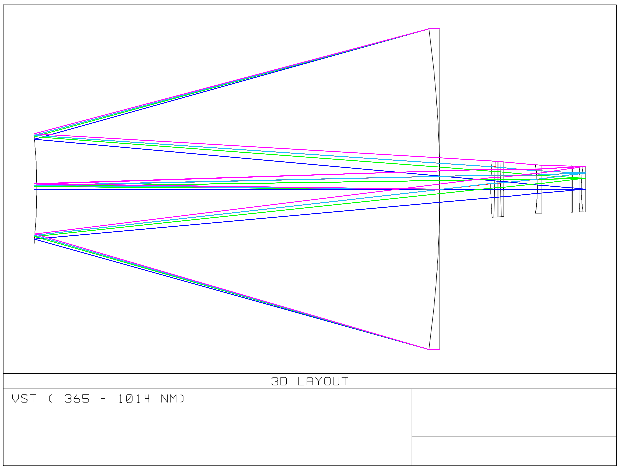

Fig. 2.1 - VST complete optical layout of telescope with one lens and the ADC, with a curve dewar window

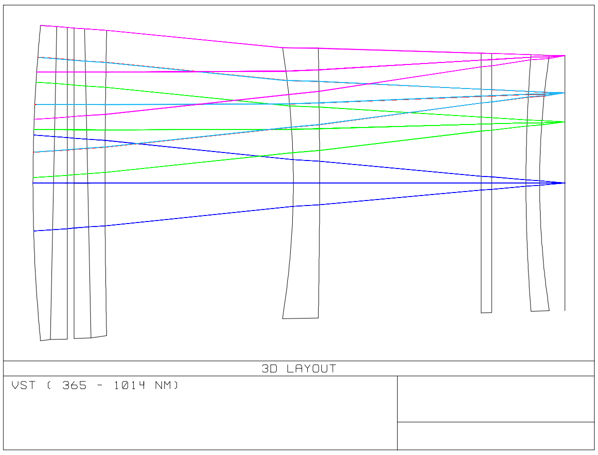

Fig. 2.2 - VST zoom of the optical layout of the corrector with one lens and the ADC, with a curve dewar window

In Fig. 2-3, 2-4 the complete optical layout of the telescope with the two lenses and the zoom of the corrector are reported.

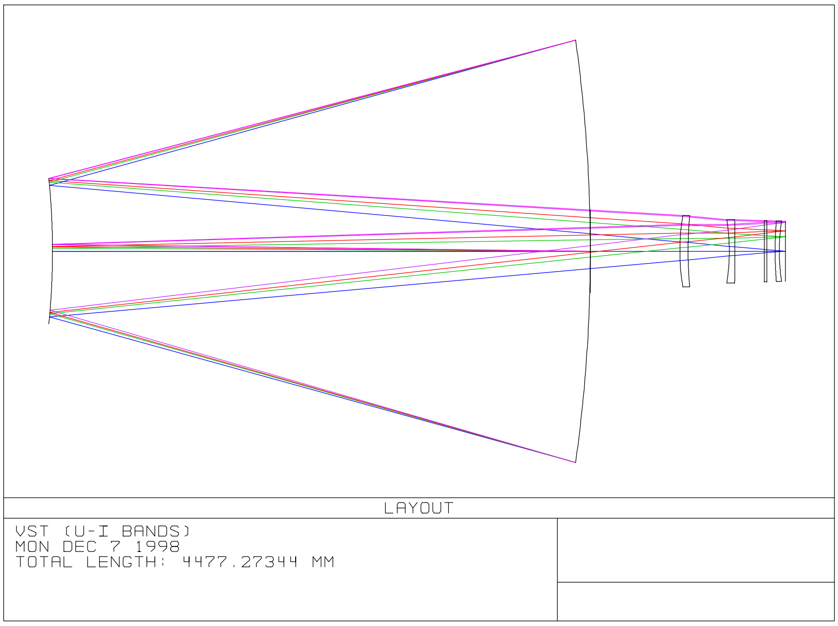

Fig.2.3 - VST optical layout of telescope with two lenses (U ÷ I bands)

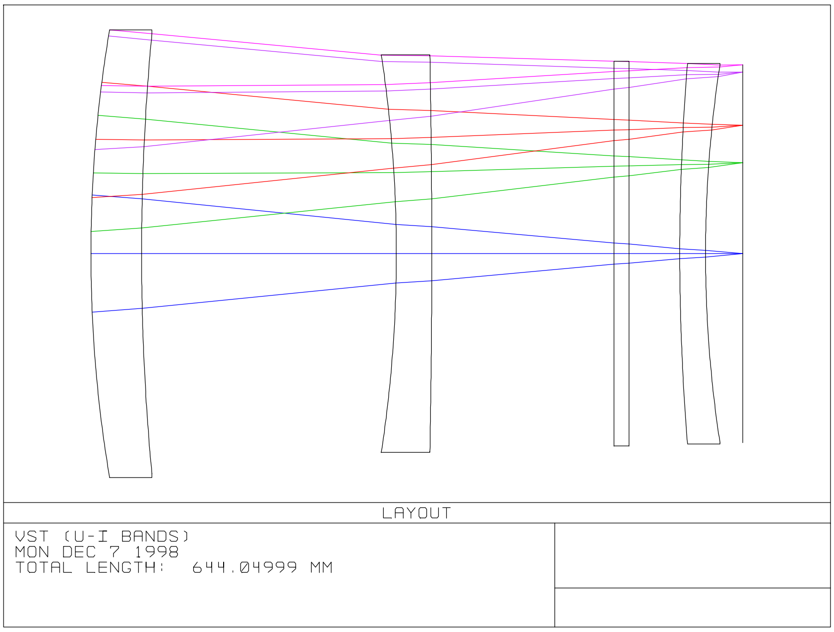

Fig.2.4 - VST zoom of the optical layout of the two lenses (U ÷ I bands)

In Tables 2.2, 2.3, 2.4, 2.5, VST main optical data, the optical data for the mirrors, the optical data with the ADC inserted and with the ADC removed are respectively shown.
The glasses of ADC were changed in order to have fixed the position of centroid of spot when observing at different angles respect to zenith. The parameters of the two correctors and of the dewar window were re-optimised in order to satisfy the mechanical constraint on the distance of last corrector element from the dewar window and, in the mean time, to keep percent distortion at low values. The distances between last corrector element and the dewar window were increased, respect to the solution of July, respectively to 290.22 mm and 245 mm, which are greater than the minimum required. All curvatures are normalised also for two lenses corrector, (see Table 2.5) and the optical quality is good. The solution found has the maximum distance achievable between last corrector element and dewar window keeping acceptable the maximum percent distortion. If the distance between last lens of the corrector with two lenses is further increased, percent distortion rises critically.

Vst Main Optical Characteristics	
Optical configuration	Modified Ritchey Chretien
Clear aperture	2610 mm
Angular field of view	1.47°
F#	5.5
Equivalent focal length	14496.93 mm (two lenses) 14395.97 mm (one lens +ADC)
Image scale	0.21 arcsec/pixel
Overall length	4477.27 mm (fixed)
Distance between mirrors	-3285.873 mm
Spectral Range	U ÷ I bands
Distance M1 vertex to first corrector lens in B, V, R, I bands	401.75 mm (>min. req.)
Distance M1 vertex to first corrector lens in U÷ I bands	547.35 mm (> min. req.)
Distance M1 vertex to CCD plane	1191.4 mm (< max. req.)
Footprint diameter of light beams in M1 centre hole	508.5 mm
Distance between last corrector element and the image plane	352.53 mm for one lens +ADC (> min. req.) 307.31 mm for two lenses (> min. req.)
Distance between last corrector element and dewar window	290.22 mm for one lens +ADC (≥ 245 mm) 245 mm for two lenses ((≥ 245 mm)
Image plane corrector in B, V, R, I bands	ADC +one lens
Atmospheric Dispersion Corrector (ADC)	Two double prisms made of PSK3 and LLF1
Image plane corrector in U÷ I bands	Two lenses
Focal Plane CCD mosaic	16 k x 16 k
CCD pixel size	15µm x 15µm

Tab. 2.2 - VST main optical data

VST MIRRORS OPTICAL DATA	
Primary Mirror parameters	
Outer Diameter	2658 mm
Clear aperture	2610 mm
Inner Diameter	600 mm
Ray of curvature	-9509 ± 4 mm
Conic constant K1	-1.139899
Secondary Mirror parameters	
Clear aperture	899.3 mm
Ray of curvature	-4374 ± 2 mm
Conic constant K2	-5.421864
Distance between mirrors	-3285.873 mm

Tab. 2.3 - VST mirrors optical data

OPTICAL DATA FOR ADC AND ONE LENS CONFIGURATION							
Element	R1	Tilt S1	R2	Tilt S2	Material	Diameter	Thickness
ADC S1,S2 (First prism)	2511.9 mm	0°	infinity	1.03°	PSK3	459.7 mm	28.57 mm
	R2	Tilt S2	R3	Tilt S3			
ADC S2,S3 (second prism)	Infinity	1.03°	infinity	0°	LLF1	457.6 mm	18.30 mm
S3,S4					Air gap		10 mm
	R4		R5				
ADC S4,S5 (third prism)	Infinity	0°	infinity	-1.03°	PSK3	452.3 mm	18.00 mm
	R5		R6				
ADC S5,S6 (fourth prism)	infinity	-1.03°	10000 mm	0°	LLF1	450.3mm	24 mm
					air		289.75 mm
L3	-1223.2		-10000		Silica	393.2 mm 391.3 mm	48.50 mm
					air		225.22 mm

Tab. 2.4 - VST optical data for ADC and one lens, in, B, V, R, I bands

OPTICAL DATA FOR TWO LENSES CONFIGURATION						
Element	R1	R2	Material	Diameter	Thickness	Air thickness
L1	1333.5 mm	2304.1 mm	Silica	441.1 mm 433.4 mm	50.00 mm	251.74 mm
L2	-1295.7 mm	-10000 mm	Silica	391.7 mm 390.3 mm	35.00 mm	180 mm
Filter	Infinity	Infinity	Silica	379.1 mm	15.00 mm	50 mm
Dewar window	2304.1 mm	1223.2 mm	Silica	374.8 mm 371.9 mm	25.45 mm	36.86 mm

Tab. 2.5 - VST optical data for two lenses corrector, filter and dewar window in U ÷ I bands

2.3.1 Shack Hartmann optical subsystem

The SH optical subsystem which is necessary for the calibration and close loop control of the active optics system is described in section 3.6.

2.4 OPTICAL PERFORMANCE

In Tables 2.6 and 2.7 the optical performance for the two configurations are reported. The optical quality is better than for solution of 06/11/98.

OPTICAL PERFORMANCE FOR THE CONFIGURATION WITH TWO LENSES (WORST CASE)	
U ÷I bands (0.320 ÷ 1.014 μm)	
Diffraction encircled energy	80 % in 1.33 pixel (at the edge of the field)
Maximum distortion	0.013 % (at the edge of the field at λ = 320 nm)
Glass transmission	99%

Tab. 2.6 - Optical performance for the configuration with two lenses

OPTICAL PERFORMANCE FOR THE CONFIGURATION WITH THE ADC AND ONE LENS (WORST CASE)	
B ÷I bands (0.365 ÷ 1.014 μm)	
Diffraction encircled energy	80 % in 1.5 pixel at zenith (at the edge of the field) 80 % in 2.88 pixel at z =70°(at the edge of the field)
Maximum distortion	0.01 % at zenith (at the edge of the field) 0.01 % at z= 70°(at the edge of the field)
Glass transmission	88 %

Tab. 2.7 - Optical performance for the configuration with the ADC and one lens

2.4.1 Encircled Energy

In Fig. 2-5, 2-6, 2-7 the curves of polychromatic diffraction encircled energy versus centroid distance, for the different fields of view are reported respectively for two lenses, ADC and one lens correctors at 0°zenith distance

The radius of the circle from centroid in which the 80% of encircled energy (normalised to diffraction limit) is enclosed is of 9.9 μm, 11.5 μm and 21.6 μm respectively for two lenses corrector and ADC and one lens corrector at 0°zenith distance and 70°zenith distance.

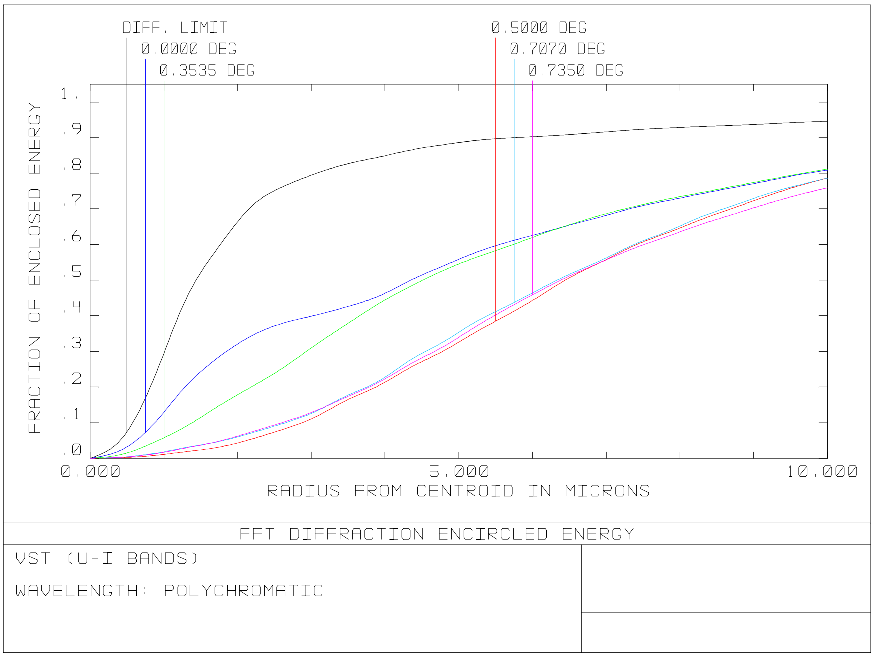

Fig.2.5 - Encircled Energy for two lenses field corrector at zenith

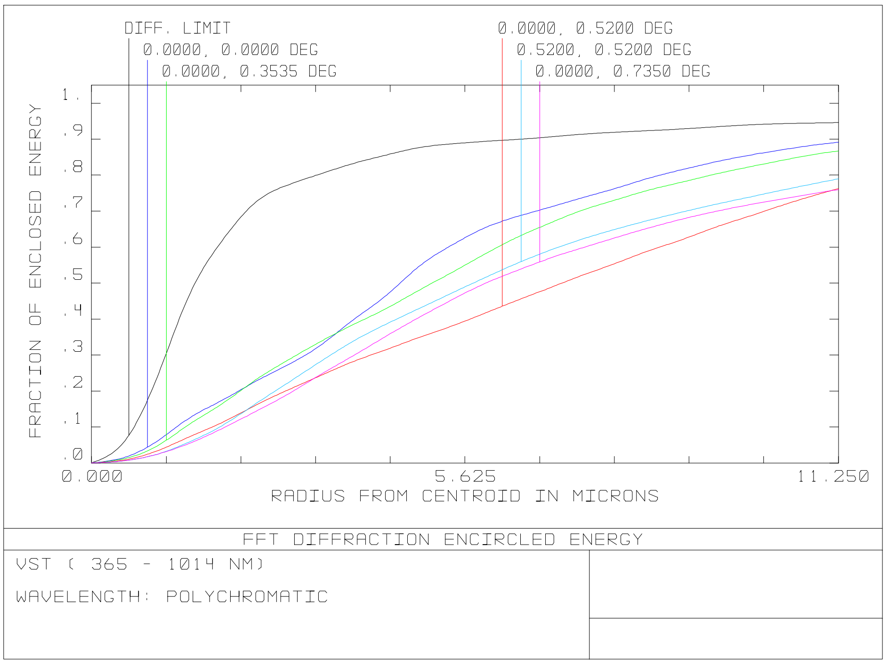

Fig.2.6 - Encircled Energy for ADC and one lens corrector at 0° zenith distance

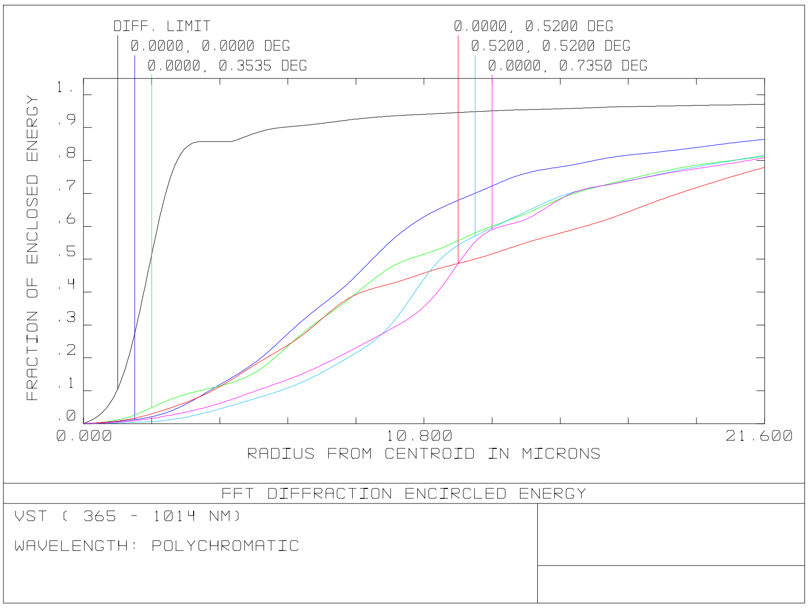

Fig.2.7 - Encircled Energy for ADC and one lens corrector at 70° zenith distance

2.4.2 Spot diagram

In Fig. 2-8÷2-10, the spot diagrams for one lens and ADC configuration at 0°, at 70° zenith distance and the spot diagrams for the configuration with two lenses at zenith are respectively shown. The configuration is that shown in Figs. 2-2 and 2-4. Note that the filters included are standard units (not interference type)

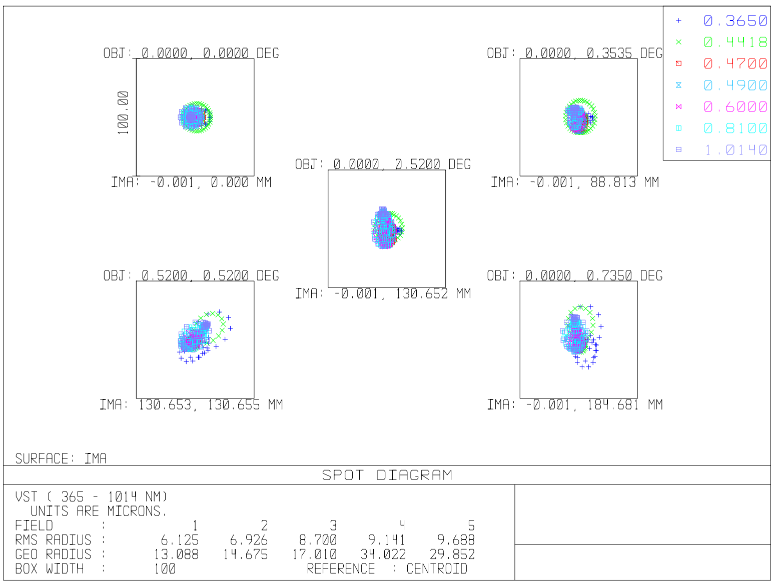

Fig.2.8 - Spot diagram for one lens and ADC at zenith from B to I

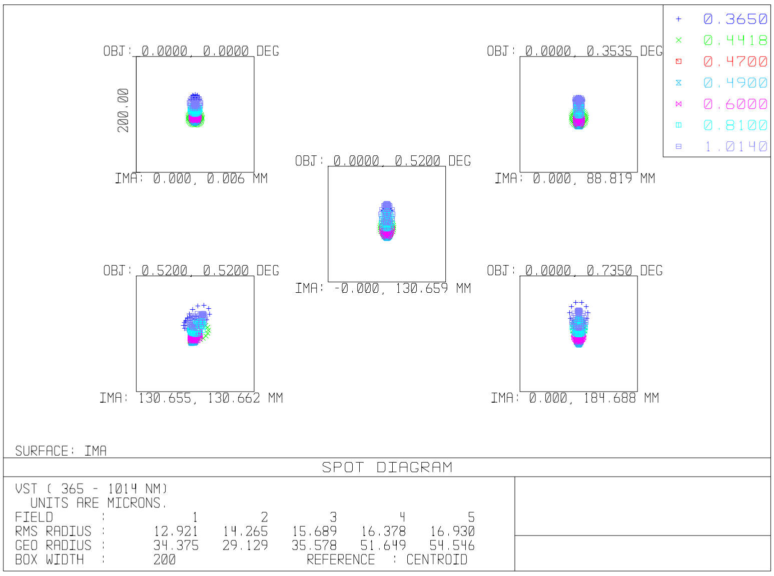

Fig.2.9 - Spot diagrams for one lens and ADC at z=70° zenith distance

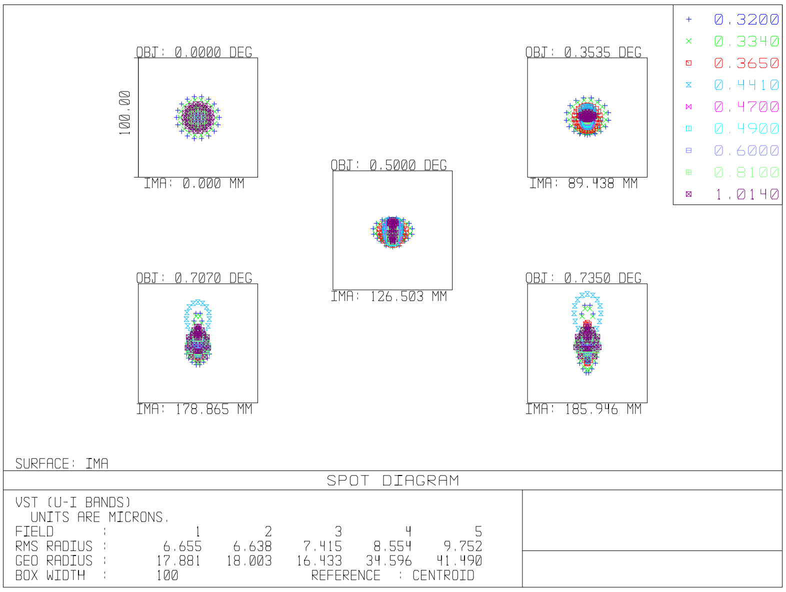

Fig.2.10 - Spot diagram for two lenses corrector from U to I bands at zenith

2.4.2.1 Spot diagram with interference filters

The spot diagrams with interference filters will be determined after the definition of the narrow band interference filters to be used in the camera.

2.4.3 MTF

In Fig. 2-11÷ 2-13 the polychromatic diffraction modulation transfer function curves for two lenses corrector and ADC and one lens corrector at 0°and 70°zenith distance are respectively shown. For two lenses corrector MTF is always greater than 58% until Nyquist frequency of 25 cycles/mm. For ADC and one lens at 0°zenith distance MTF is always greater than 58% until Nyquist frequency of 22.22 cycles/mm, and at 70°zenith distance is greater than 40.7% until Nyquist frequency of 13.33 cycles/mm.

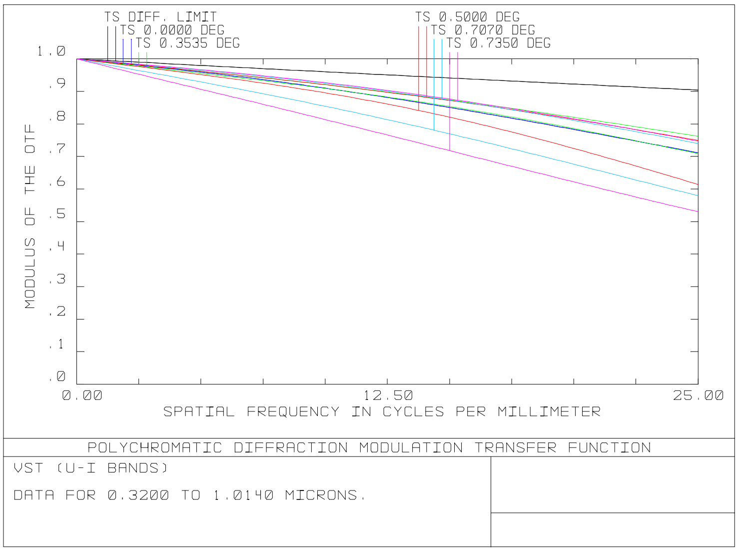

Fig.2.11 - MTF two lenses field corrector at zenith

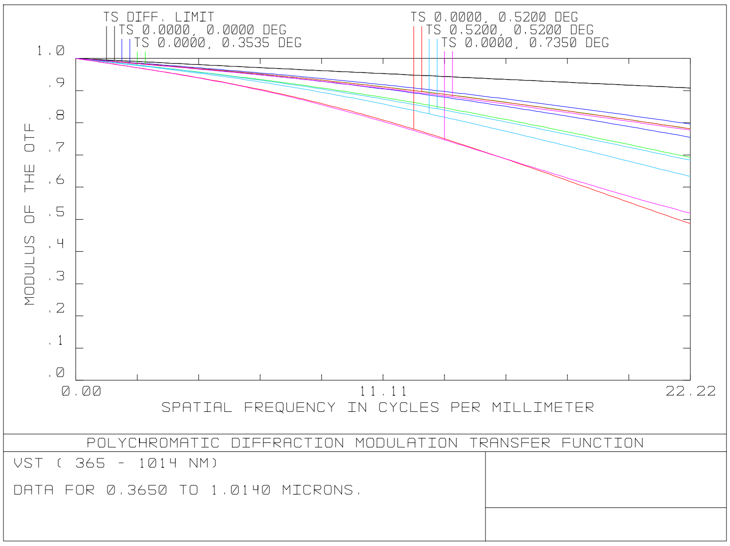

Fig.2.12 - MTF ADC an one lens corrector at 0° zenith distance

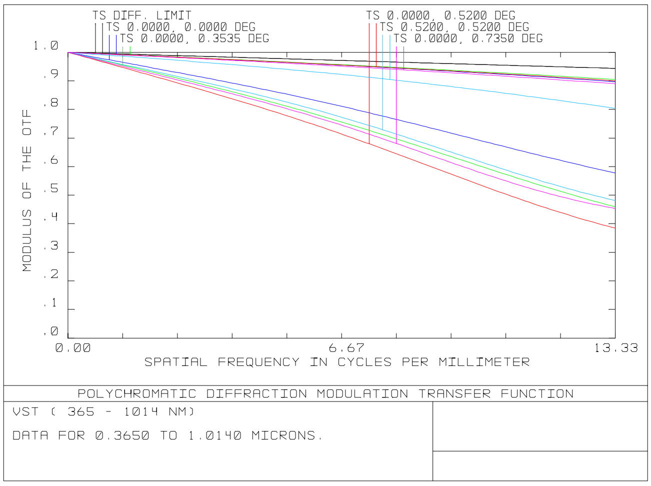

Fig.2.13 - MTF ADC an one lens corrector at 70° zenith distance

2.4.4 Field curvature and distortion curves

In Figures 2-14, 2-15 the field curvature and distortion curves for the configurations with ADC and one lens at 70° zenith distance and with two lenses are respectively reported. For the ADC and one lens corrector at 70°zenith distance the maximum distortion is 0.01 %, at the edge of the field for λ =1.014 μm. For two lenses corrector the maximum distortion is 0.013% at the edge of the field for λ =0.32 μm. The focal plane is flat and it is located in the origin of field curvature diagram between tangential and sagittal curves. The field curvature plot shows the distance from the currently defined focal plane(origin of the graphic) to the paraxial focal plane as function of field view. The plane in which field curvature is zero is the image plane chosen for the system where there is the best focus and the radius in which 80% of encircled energy is enclosed is minimised. The field curvature curves for the tangential and sagittal rays are defined as the distances from the defined image plane of best focus to the paraxial focal planes for those rays, for each field of view. The best focus image plane is the focal plane in which the diameter of spot diagram is minimised and optimised for all the fields of view and is not necessarily coincident with the paraxial focal planes as described in Figs.2.14 and 2.15

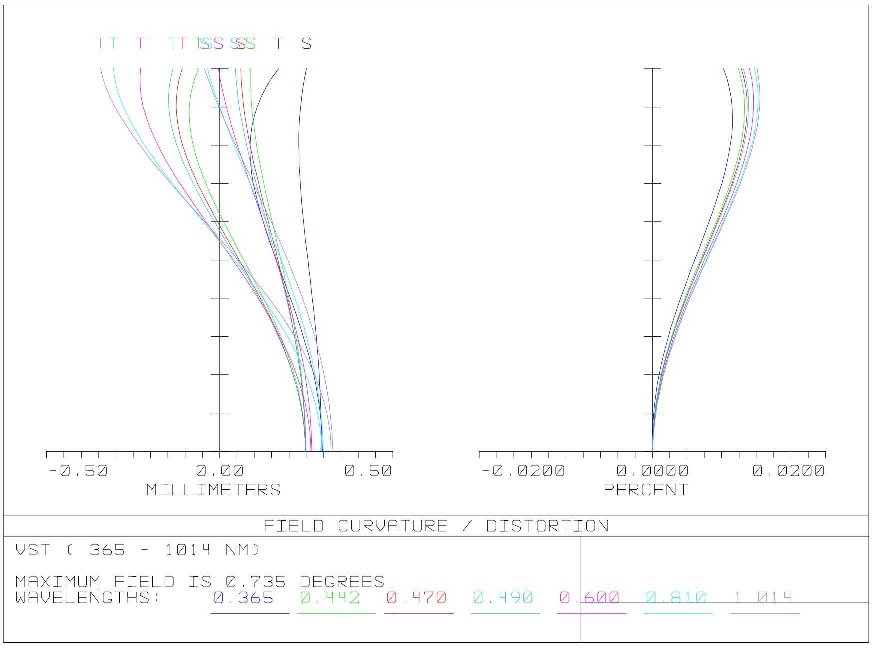

Fig.2.14 - Field curvature and distortion curves for the configuration with one lens and ADC at z angle of 70° zenith distance

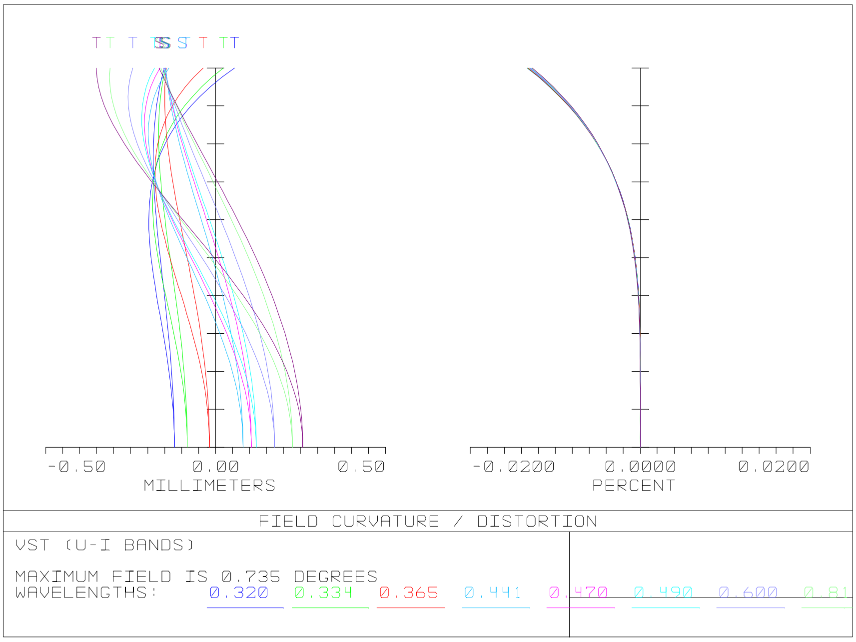

Fig.2.15 - Field curvature and distortion curves for the configuration with two lenses

2.4.5 Analysis of focus depth

The analysis of focus depth for two correctors configurations was performed. The depth of focus was calculated respect the best focus image plane of the optical system which is the plane in which field curvature is zero and the radius in which 80% of encircled energy is enclosed is minimised, as discussed in section 2.4.4.
In Tables 2.8, 2.9, 2.10 the depth of focus calculated for the two correctors are reported.

Depth of focus	EE% variation with respect to EE 80%
+ 10 μm	-2.5%
- 10 μm	0%
+ 20 μm	-2.8%
- 20 μm	+0%
+ 30 μm	-6.5%
- 30 μm	0%

Tab. 2.8 - Depth of focus versus EE % variation for the configuration with the ADC and one lens at 70° zenith angle

Depth of focus	EE% variation with respect to EE 80%
+ 10 μm	0%
- 10 μm	0 %
+ 20 μm	6.2%
- 20 μm	0 %
+ 30 μm	0 %
- 30 μm	0 %

Tab. 2.9 - Depth of focus versus EE % variation for the configuration with the ADC and one lens at 0° zenith angle

Depth of focus	EE% variation with respect to EE 80%
+ 10 μm	0%
- 10 μm	0%
+ 20 μm	0%
- 20 μm	-2.25 %
+ 30 μm	-4.5 %
- 30 μm	-4.2 %

Tab. 2.10 - Depth of focus versus EE % variation for the configuration with the two lenses at zenith

2.5 EFFICIENCY CURVES FOR THE TWO CONFIGURATIONS

In Fig. 2-16, 2-17 the efficiency curves for the two configurations are shown. It was considered a filter of Silica (SQ1 from Zeiss) 15 mm thick and a dewar window of Silica 25.45 mm thick. The coating of the mirrors is aluminium and that one of the correctors is AR coating measured from Zeiss which has a transmission better than 0.985.

2.5.1 Efficiency with ADC and one lens field corrector

In Fig.2-16 the curves of efficiency for VST, for ADC and one lens corrector are shown. The highest curve shows the corrector (PSK3, LLF1, Silica SQ1) with coating efficiency. The maximum residual reflectance for coating measured from Zeiss, (which is less than 1.5% over the whole range from 365 to 1014 nm) was considered.
The second curve and the third one from the top are respectively the aluminium coating reflectivity of the two mirrors and the efficiency of corrector with a filter of Silica 15 mm thick, a dewar window of Silica 25.45 mm thick, with corrector coating. The fourth and the fifth are the total efficiencies of the telescope, respectively with and without filter, taking into account, corrector, dewar window, corrector coating and mirrors coating. The last curve downwards is the total efficiency of the telescope with filter, taking into account also the M2 baffle obscuration, which is of 17%.
The total efficiency is over 63% without M2 baffle obscuration, and over 52% with baffling the range 365 ÷ 1014.

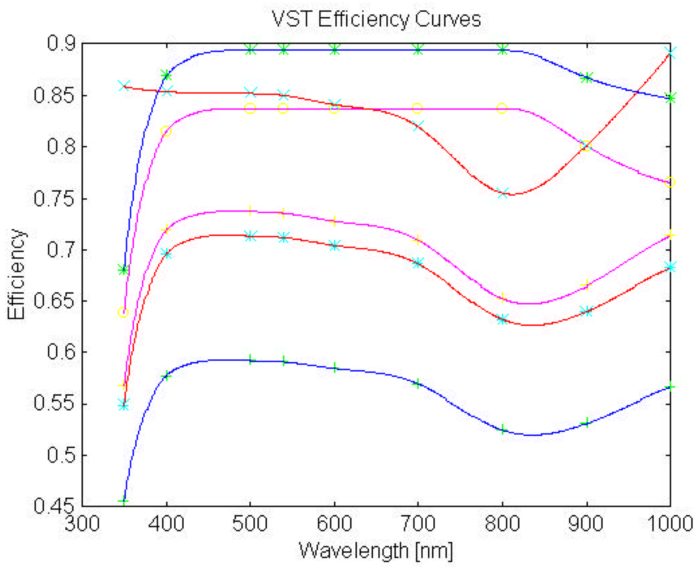

Fig.2.16 - Efficiency curves for ADC and one lens corrector at z=0

(* green) Corrector with AR wideband multilayer coating measured from Zeiss (R<1.5%)
(x cyan) Mirrors coated with aluminium
(o yellow) Corrector with filter and dewar window, with coating
(+ yellow) Total efficiency (telescope + corrector + dewar window, with coating)
(* ciano) Total efficiency (telescope + corrector +filter+ dewar window with coating
(+ green) Total efficiency (telescope + corrector + dewar window + filter, + M2 baffle obscuration, with coating)
.

2.5.2 Efficiency with two lenses field corrector

In Fig.2-17 the curves of efficiency for VST, for two lenses corrector are shown. The highest curve shows corrector (Silica SQ1 from) with coating efficiency. The maximum residual reflectance for coating measured from Zeiss, (which is less than 1.5% over the whole range from 320 to 1014 nm) was considered.
The second curve and the third one from the top are respectively the aluminium coating reflectivity of the two mirrors and the efficiency of corrector with a filter of Silica 15 mm thick, a dewar window of Silica 25.45 mm thick, with coating.
The fourth and the fifth are the total efficiencies of the telescope, respectively with and without filter, taking into account, corrector, dewar window, corrector coating and mirrors coating. The last curve downwards is the total efficiency of the telescope with filter, taking into account also the M2 baffle oscuration, which is of 17%. The total efficiency is over 66% without M2 baffle obscuration, and over 55% with baffle in the range 320 ÷1014 nm.

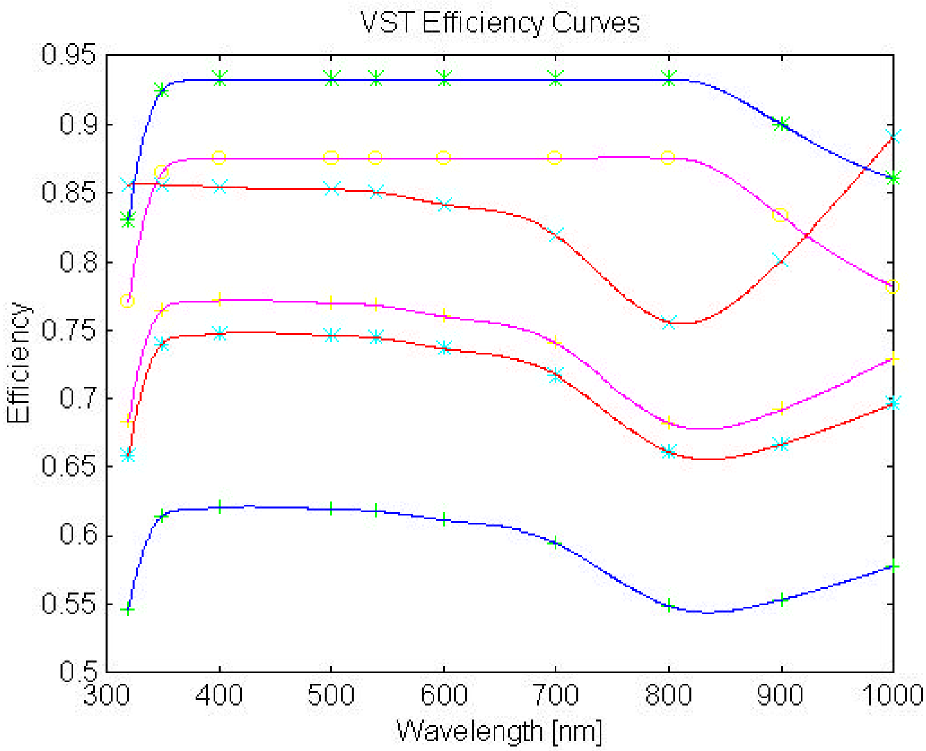

Fig.2.17 - Efficiency curves for two lenses corrector

(* green) Corrector with AR wideband multilayer coating measured from Zeiss (R<1.5%)
(x cyan) Mirrors coated with aluminium
(o yellow) Corrector with filter and dewar window, with coating
(+ yellow) Total efficiency (telescope + corrector + dewar window + filter, with coating)
(* ciano) Total efficiency (telescope + corrector +filter+ dewar window with coating
(+ green) Total efficiency (telescope + corrector + dewar window + filter, + M2 baffle obscuration, with coating)

2.6 Ghost Analysis

The ghost analysis has been performed using paraxial rays. This method can be used to select the most critical ghosts. Two kind of ghost image were analysed: the bright focused ghost image and the sky concentration effects..

2.6.1 Ghost analysis with ADC and one lens field corrector

Each surface has a number according to Fig. 2-18, which was used in the analysis. In addition surfaces 1, 2, 3 are respectively M1, M2, the dummy surface at the primary hole.
The analysis was limited to two reflections. In the Table 2.11 are reported all possible ghosts. The analysis was done at z =0.

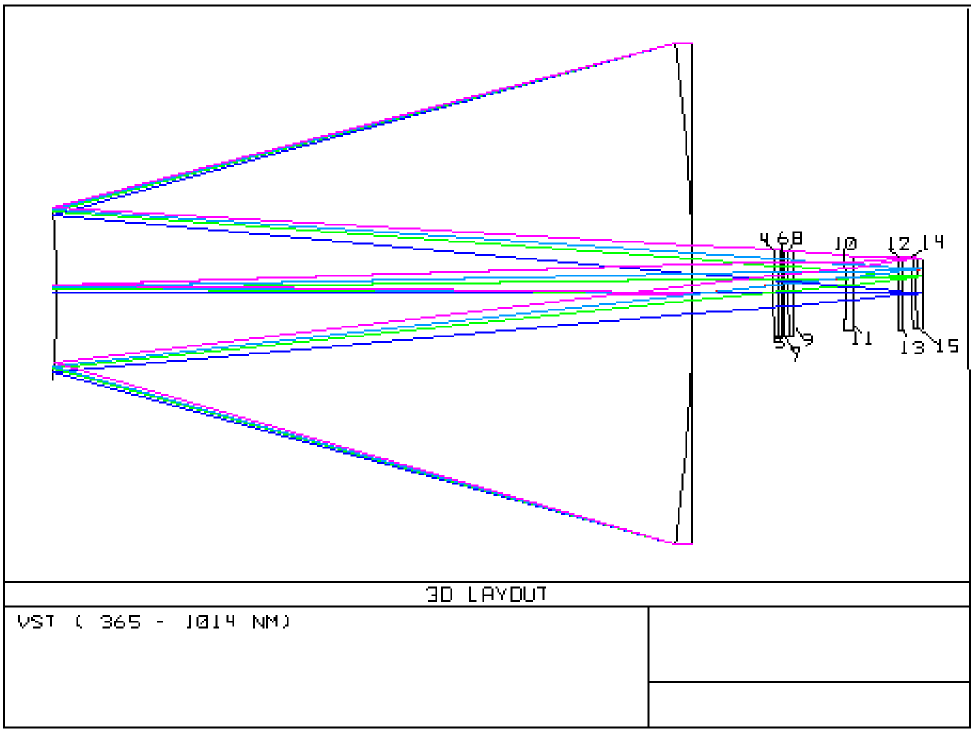

Fig.2.18 - ADC and one lens

Ghost analysis for ADC and one lens field corrector configuration (365 ÷ 1014 nm)						
REFL 1	REFL 2	DBFL	EFL	DISC	PUPIL RATIO	MAGNIFICATION
2	1	-1991.172780	-323.209465	-1297.755810	1.000000	0.139085
4	1	-2100.092044	-17.892368	-846.559076	1.000000	0.224877
5	1	-2107.840192	186.984105	-4235.981959	1.031508	0.045107
6	1	-2107.905413	187.103355	-4230.830973	1.030939	0.045164
7	1	-2107.961226	187.205287	-4226.433263	1.030453	0.045212
8	1	-2108.025674	187.322859	-4221.366723	1.029893	0.045268
9	1	-2107.726204	-100.623175	-3449.590186	1.000000	0.055387
10	1	-2110.077621	12.527290	-6080.178130	1.514327	0.031459
11	1	-2109.779097	-43.070152	-3390.593327	1.000000	0.056406
12	1	-2111.130599	-27.985027	-3680.223997	1.000000	0.052000
13	1	-2111.185905	-27.897014	-3704.346320	1.000000	0.051663
14	1	-2111.439355	-11.290180	-3638.159443	1.000000	0.052609
15	1	-2111.525891	-6.381744	-3576.343203	1.000000	0.053521
16	1	-2111.711344	-16.919505	-3949.890632	1.000000	0.048463
4	2	-1964.466672	-41.842709	-315.633990	1.000000	0.564190
5	2	-2011.078450	524.942616	-1685.495091	1.000000	0.108160
6	2	-2011.453305	525.217576	-1684.334548	1.000000	0.108254
7	2	-2011.773861	525.452554	-1683.343721	1.000000	0.108335
8	2	-2012.143764	525.723529	-1682.202204	1.000000	0.108429
9	2	-2010.422639	-220.192727	-1371.323231	1.000000	0.132896
10	2	-2023.780366	29.860164	-2463.084336	1.000000	0.074481
11	2	-2022.104206	-98.067405	-1370.276985	1.000000	0.133770
12	2	-2029.647838	-64.277027	-1503.314174	1.000000	0.122387
13	2	-2029.954107	-64.070334	-1513.825787	1.000000	0.121555
14	2	-2031.355196	-26.262096	-1489.738862	1.000000	0.123606
15	2	-2031.832667	-14.900545	-1465.420296	1.000000	0.125687
16	2	-2032.854358	-39.148990	-1620.834462	1.000000	0.113693
5	4	-350.689651	362.515387	-69.188686	1.000000	0.459465
6	4	-357.530997	362.942539	-69.685119	1.000000	0.465091
7	4	-363.505859	363.308023	-70.108954	1.000000	0.470005
8	4	-370.547852	363.730005	-70.597248	1.000000	0.475796
9	4	-339.083198	571.987557	-55.516732	1.000000	0.553664
10	4	-720.750687	154.468641	-127.903728	1.000000	0.510818
11	4	-647.823333	800.209320	-69.199708	1.000000	0.848627
12	4	-1106.123871	1010.728635	-85.550020	1.000000	1.172055
13	4	-1134.805778	999.896207	-86.540473	1.000000	1.188684
14	4	-1283.122686	-1139.522729	-86.927947	1.000000	1.338052
15	4	-1341.191428	-304.027194	-86.099866	1.000000	1.412058
16	4	-1481.509286	2952.436445	-96.628683	1.000000	1.389833
6	5	-31.226640	-698.496850	-2.877272	1.000000	0.983804
7	5	-57.320664	-699.343435	-5.354647	1.000000	0.970386
8	5	-86.514483	-700.321321	-8.208796	1.000000	0.955375
9	5	58.084009	-401.442990	4.155146	1.000000	1.267169
10	5	-683.471232	216.316258	-142.872288	1.000000	0.433647
11	5	-623.733602	-270.723498	-69.049360	1.000000	0.818849
12	5	-853.317139	-200.619242	-127.122845	1.000000	0.608487
13	5	-860.830542	-199.760696	-130.103779	1.000000	0.599780
14	5	-893.800806	-101.439594	-137.443975	1.000000	0.589494
15	5	-904.538278	-61.965719	-138.351966	1.000000	0.592660
16	5	-926.720247	-137.526645	-160.478365	1.000000	0.523476
7	6	-26.684485	-698.352046	-2.452927	1.000000	0.986140
8	6	-56.826308	-699.327159	-5.307076	1.000000	0.970641
9	6	92.616060	-403.020042	6.513145	1.000000	1.289021
10	6	-669.865738	219.182911	-138.533484	1.000000	0.438326
11	6	-608.800848	-272.220177	-66.642756	1.000000	0.828107
12	6	-843.144734	-201.852092	-124.447219	1.000000	0.614160
13	6	-850.798391	-200.987131	-127.408003	1.000000	0.605333
14	6	-884.372499	-102.191852	-134.784613	1.000000	0.594784
15	6	-895.302544	-62.456738	-135.733846	1.000000	0.597924
16	6	-917.875994	-138.464049	-157.577450	1.000000	0.528025
8	7	-30.718516	-698.480614	-2.829701	1.000000	0.984065
9	7	123.054701	-404.376306	8.526313	1.000000	1.308282
10	7	-658.015405	221.691160	-134.829183	1.000000	0.442401
11	7	-595.782028	-273.511141	-64.588092	1.000000	0.836179

REFL 1	REFL 2	DBFL	EFL	DISC	PUPIL RATIO	MAGNIFICATION
12	7	-834.308635	-202.916705	-122.162874	1.000000	0.619087
13	7	-842.085166	-202.046194	-125.106456	1.000000	0.610156
14	7	-876.188040	-102.842986	-132.514154	1.000000	0.599376
15	7	-887.286626	-62.882151	-133.498598	1.000000	0.602492
16	7	-910.202566	-139.274539	-155.100762	1.000000	0.531972
9	8	159.270073	-405.950198	10.845656	1.000000	1.331198
10	8	-644.086673	224.652996	-130.561509	1.000000	0.447191
11	8	-580.465029	-275.013706	-62.220942	1.000000	0.845676
12	8	-823.951275	-204.157238	-119.531112	1.000000	0.624863
13	8	-831.873071	-203.280245	-122.454875	1.000000	0.615808
14	8	-866.600763	-103.603510	-129.898390	1.000000	0.604755
15	8	-877.898400	-63.379504	-130.923399	1.000000	0.607843
16	8	-901.218672	-140.220136	-152.247405	1.000000	0.536592
10	9	-626.162223	203.739810	-122.278364	1.000000	0.464196
11	9	-559.622110	-410.428339	-59.536712	1.000000	0.852068
12	9	-838.081943	-289.933093	-107.114518	1.000000	0.709255
13	9	-848.330211	-288.817023	-109.565718	1.000000	0.701867
14	9	-894.275104	-133.747108	-115.479202	1.000000	0.701991
15	9	-909.589765	-78.937952	-116.158478	1.000000	0.709838
16	9	-941.794395	-189.148584	-134.542277	1.000000	0.634544
11	10	497.196780	-133.038975	15.258352	1.000000	2.953826
12	10	-445.613126	-108.658339	-58.313474	1.000000	0.692713
13	10	-455.137162	-108.091345	-61.777799	1.000000	0.667843
14	10	-492.429776	-69.547847	-74.543706	1.000000	0.598822
15	10	-503.202064	-47.529634	-77.931521	1.000000	0.585320
16	10	-523.664137	-83.783815	-97.086486	1.000000	0.488943
12	11	-417.245965	-461.891789	-41.741636	1.000000	0.906123
13	11	-434.027730	-460.367627	-43.734547	1.000000	0.899616
14	11	-510.632790	-191.625087	-50.690166	1.000000	0.913165
15	11	-536.676458	-109.228119	-52.425279	1.000000	0.927975
16	11	-592.298783	-283.824157	-64.045680	1.000000	0.838331
13	12	-20.242610	-695.920251	-1.841661	1.000000	0.996371
14	12	-115.771814	-243.746227	-10.207117	1.000000	1.028168
15	12	-148.975767	-132.548444	-12.852007	1.000000	1.050773
16	12	-221.168242	-386.808691	-20.864206	1.000000	0.960915
14	13	-95.950698	-244.498908	-8.429393	1.000000	1.031849
15	13	-129.392113	-132.983872	-11.122959	1.000000	1.054513
16	13	-202.095923	-387.884806	-18.998275	1.000000	0.964290
15	14	-32.074097	-213.350208	-2.762768	1.000000	1.052384
16	14	-109.494861	5318.830946	-9.646562	1.000000	1.028929
16	15	-75.778694	277.555902	-6.458313	1.000000	1.063634

Tab. 2.11 - Table of all possible ghosts for ADC and one lens corrector configuration

Keys to Tab. 2.11:

- REFL1 - is the number of the surface on which the light is reflected for the 1st time
- REFL2 - is the number of the surface on which the light is reflected for the 2nd time
- DBFL - (Delta Back Focal Length) is the distance (mm) from the primary image plane to the reflected image. This is a measure of how far out of focus the ghost image is for this surface pair. If the DBFL is near zero, then the ghost image will be nearly in focus.
- EFL - (Effective Focal Length) is the focal length (mm) of the system including the two extraneous reflections. This allows to compute the size of the ghost image at the focal plane location indicated by DBFL.
- DISC - is the semi-diameter (mm) of the reflected beam (from an on-axis object point) at the primary image plane. The smaller this number is, the nearer the ghost image is to being in focus. This will usually only be small when DBFL is also small.
- PUPIL RATIO - is the maximum ratio of the first order reflected ray heights at the stop surface to the stop semi-diameter. The paraxial marginal ray will pass through the stop surface either once or three times, depending on whether the stop surface is between the reflecting pair of surface or not. If on any of these passes the paraxial ray at the stop surface is larger than the stop diameter, then this ratio will be greater than unity. Since there is by definition an aperture on the stop surface which will limit the rays to the stop diameter, intensity values of ghost images will be reduced for surface pairs whose pupil ratio is greater than unity.
- MAGNIFICATION - is the size of the reflected image at the image plane indicated by DBFL relative to the size of the primary image. It is the ratio of the EFL, with the reflections, to the nominal EFL of the system.

2.6.2 Ghost analysis with two lenses field corrector

Each surface has a number according to Fig. 2-19, which was used in the analysis. In addition surfaces 1, 2, 3 are respectively M1, M2, the dummy surface at the primary hole. The analysis has been limited also to two reflections. In the Table 2.12 are reported all possible ghosts.

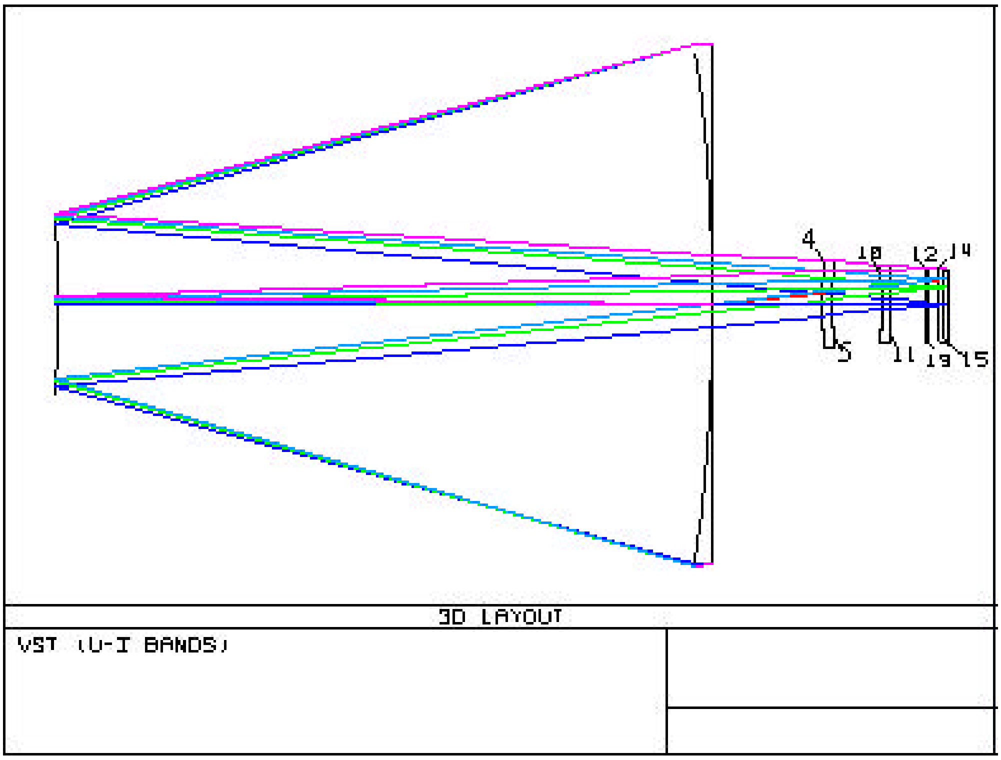

Fig.2.19 - Two lenses corrector

Ghost analysis for two lenses field corrector configuration (320 ÷ 1014 nm)

REFL 1	REFL 2	DBFL	EFL	DISC	PUPIL RATIO	MAGNIFICATION
2	1	-1970.493875	-317.080495	-1306.947915	1.000000	0.135730
4	1	-2113.336142	-10.368946	225.250033	1.000000	-0.844624
5	1	-2082.384788	-21.447080	-2065.037356	1.000000	0.090781
10	1	-2085.380286	12.601743	-5707.512689	1.414963	0.032893
11	1	-2085.168795	-40.829024	-3487.213915	1.000000	0.053830
12	1	-2086.167836	-26.849986	-3704.905649	1.000000	0.050691
13	1	-2086.220097	-26.765261	-3729.273599	1.000000	0.050361
14	1	-2086.460971	-10.887308	-3664.945549	1.000000	0.051251
15	1	-2086.542686	-6.148948	-3602.817781	1.000000	0.052137
16	1	-2086.718682	-16.174642	-3978.887906	1.000009	0.047213
4	2	-2137.686018	-24.360107	112.170391	1.000000	-1.715638
5	2	-1986.209115	-49.892760	-817.498766	1.000000	0.218725
10	2	-2003.290531	30.049373	-2316.624408	1.000000	0.077848
11	2	-2002.104394	-93.063444	-1412.964212	1.000000	0.127560
12	2	-2007.681516	-61.745716	-1513.522402	1.000000	0.119417
13	2	-2007.971460	-61.546553	-1524.127282	1.000000	0.118603
14	2	-2009.305522	-25.350725	-1500.781201	1.000000	0.120528
15	2	-2009.757234	-14.371253	-1476.321872	1.000000	0.122553
16	2	-2010.728662	-37.469404	-1632.758561	1.000000	0.110864
5	4	-241.135825	547.628499	-36.341242	1.000000	0.597340
10	4	-596.133624	130.974133	-90.589447	1.000000	0.592415
11	4	-535.024835	266.107209	-55.773421	1.000000	0.863588
12	4	-1066.359776	259.539255	-57.125586	1.000000	1.680478
13	4	-1127.188882	257.738406	-57.389238	1.000000	1.768178
14	4	-1535.229059	319.722763	-55.891728	1.000000	2.472780
15	4	-1753.112116	459.645417	-54.775012	1.000000	2.881291
16	4	-2535.716424	258.623945	-60.090029	1.000000	3.798902
10	5	-542.867299	171.593555	-90.311958	1.000000	0.541138
11	5	-487.552918	9720.041296	-51.288871	1.000000	0.855773
12	5	-787.802687	-2367.153634	-74.008573	1.000000	0.958286
13	5	-806.666296	-2385.461108	-75.522553	1.000000	0.961562
14	5	-898.717367	-330.658045	-78.871951	1.000000	1.025795
15	5	-931.997547	-156.239021	-79.086120	1.000000	1.060900
16	5	-1007.580487	-672.090705	-91.030562	1.000000	0.996443
11	10	264.514759	-137.777081	10.752659	1.000000	2.214593
12	10	-369.135282	-115.073661	-42.522498	1.000000	0.781496
13	10	-381.163234	-114.466780	-45.641321	1.000000	0.751818
14	10	-428.006426	-74.658033	-57.712203	1.000000	0.667640
15	10	-441.298865	-51.342928	-61.021287	1.000000	0.651045
16	10	-466.494291	-88.995030	-77.587694	1.000000	0.541269
12	11	-339.311384	-460.498992	-32.961023	1.000000	0.926739
13	11	-356.764412	-458.962123	-34.912472	1.000000	0.919943
14	11	-436.832880	-192.926718	-42.166327	1.000000	0.932630
15	11	-463.856955	-110.050076	-44.071049	1.000000	0.947525
16	11	-521.825086	-282.765547	-54.901360	1.000000	0.855661
13	12	-20.405750	-682.838726	-1.843785	1.000000	0.996327
14	12	-115.939271	-240.958849	-10.158464	1.000000	1.027454
15	12	-148.929636	-130.949797	-12.769301	1.000000	1.049963
16	12	-221.012814	-378.444550	-20.721171	1.000000	0.960203
14	13	-96.242296	-241.710126	-8.402203	1.000000	1.031176
15	13	-129.471362	-131.384554	-11.061117	1.000000	1.053743
16	13	-202.071015	-379.508722	-18.878217	1.000000	0.963614
15	14	-32.184569	-210.241386	-2.753825	1.000000	1.052134
16	14	-109.567484	6538.841855	-9.588810	1.000000	1.028672
16	15	-76.094493	276.845963	-6.437393	1.000000	1.064151

Tab. 2.12 - Table of all possible ghosts for two lenses corrector configuration

2.6.3 Analysis of focused ghosts

The brightest focused ghosts are reported in Table 2.13.

ADC and one lens corrector							
REFL 1	REFL 2	DBFL	EFL	DISC	GHOST AREA (mm^2)	PUPIL RATIO	MAGNIFICATION
7	6	-26.684485	-698.352046	-2.452927	18.86	1.000000	0.986140
13	12	-20.242610	-695.920251	-1.841661	10.6	1.000000	0.996371
15	14	-32.074097	-213.350208	-2.762768	23.93	1.000000	1.052384
Two lenses corrector							
REFL 1	REFL 2	DBFL	EFL	DISC	GHOST AREA (mm^2)	PUPIL RATIO	MAGNIFICATION
13	12	-20.405750	-682.838726	-1.843785	10.64	1.000000	0.996327
15	14	-32.184569	-210.241386	-2.753825	23.76	1.000000	1.052134

Tab. 2.13 - Summary of the brightest focused ghosts

2.6.4 Analysis of sky concentration

The sky concentration is a small image of the telescope pupil located near the detector. The combinations which may create sky concentration which is the pupil ghost are reported in Table 2.14. They are due to reflections between CCD and the back surface of the dewar window.

ADC and One lens corrector							
REFL 1	REFL 2	DBFL	EFL	DISC	GHOST AREA (mm^2)	PUPIL RATIO	MAGNIFICATION
16	15	-75.778694	277.555902	-6.458313	131	1.000000	1.063634
Two lenses corrector							
REFL 1	REFL 2	DBFL	EFL	DISC	GHOST AREA (mm^2)	PUPIL RATIO	MAGNIFICATION
16	15	-76.094493	276.845963	-6.437393	130.2	1.000000	1.064151

Tab. 2.14 - Summary of most focalised ghost for sky concentration

2.6.5 Ghost analysis summary

The first brightest focused ghost is generated between the two flat and parallel surfaces of the ADC, in the region which divide the two couples of thin prisms. The second and third ghosts are generated between the two faces of the filter and dewar window and are present in both optical configurations. The pupil ghost which is the sky concentration is created by the reflections between CCD and the back surface of the dewar window.

The maximum area of ghost image and optical system image ratio for the most focalised ghosts is of order of 10^{-4}, while for sky concentration is of order of 10^{-5}.They are negligible and are calculated considering two reflections so they can be reduced of a factor 10^{4} when the two reflecting surfaces are coated with a multilayer wideband coating like that proposed by Zeiss.

2.7 OPTICAL TOLERANCES

A preliminary study of the tolerances of the two systems is presented. In the following Tables 2.15, 2.16 the centred tolerance for the two lenses corrector and for ADC and one lens corrector are reported. Radius, radius tolerance, thickness and thickness tolerance are given in mm. Fringes of power and irregularity are at 546.1 nm over the clear aperture. Irregularity is defined as fringes of cylinder power in test plate fit.

Centred tolerances for two lenses field corrector

Surface	Radius	Radius Tol	Fringes Pow/Irr	Thickness	Thickness Tol	Glass	Index Tol	V-NO (%)
1	-9509.00000	4.0000	4.0/ 0.25	-3285.87337		REFL		
2	-4374.00000	2.0000	4.0/ 0.25	3285.87337		REFL		
3				547.35000	0.50000			
4	1333.50000	0.1000	4.0/ 4.00	50.00000	0.25000	SILICA	0.00100	0.04
5	2304.10000	0.1000	4.0/ 4.00	0.00000		AIR		
6			4.0	0.00000		AIR		
7			4.0	0.00000		AIR		
8			4.0	0.00000		AIR		
9			4.0	251.74000	0.50000	AIR		
10	-1295.70000	1.0000	4.0/ 4.00	35.00000	0.25000	SILICA		0.04
11	-10000.00000	1.5000	4.0/ 6.00	180.00000	1.00000	AIR		
12	INF		4.0	15.00000	0.05000	SILICA		0.04
13	INF		4.0	50.00000	0.08000			
14	2304.10000	1.0000	4.0/ 6.00	25.45000	0.05000	SILICA		0.04
15	1223.20000	0.7000	4.0/ 6.00	36.86000	0.05000			

Tab. 2.15 - Centred tolerances for two lenses field corrector

Centred tolerances for one lens field corrector and ADC

Surface	Radius	Radius Tol	Fringes Pow/Irr	Thickness	Thickness Tol	Glass	Index Tol	V-NO (%)
1	-9509.00000	4.0000	4.0/ 0.25	-3285.87337		REFL		
2	-4374.00000	2.0000	4.0/ 0.25	3285.87337		REFL		
3				415.60000	0.50000			
4	2371.40000	0.1000	4.0/ 4.00	30.00000	0.25000	BK7	0.00100	0.04
5	INF		4.0/ 4.00	20.00000	0.05000	LLF6	0.00200	0.04
6	INF		4.0	10.00000	0.05000	AIR		
7	INF		4.0	20.00000	0.05000	BK7		0.04
8	INF		4.0	25.00000	0.05000	LLF6	0.00200	0.04
9	10000.00000	0.1000	4.0/ 4.00	274.24000	0.50000	AIR		
10	-1223.20000	0.5000	4.0/ 4.00	38.28000	0.25000	SILICA	0.00100	0.04
11	-10000.00000	1.5000	4.0/ 6.00	235.53000	0.30000	AIR		
12	INF		4.0	15.00000	0.05000	SILICA		0.04
13	INF		4.0	50.00000	0.08000			
14	2304.10000	1.0000	4.0/ 6.00	20.00000	0.05000	SILICA		0.04
15	1223.20000	0.7000	4.0/ 6.00	36.69000	0.05000			
16				0.00000				

Tab. 2.16 - Centred tolerances for one lens field corrector and ADC

In Table 2.17 and Table 2.18 the de-centred tolerances for the two optical configuration are respectively reported. Radii are given in units of mm. For wedge and tilt, TIR is a single indicator measurement taken at the smaller of the two clear apertures. For decentre and roll, TIR is a measurement of the induced wedge and is the maximum difference in readings between two indicators, one for each surface, with both surfaces measured at their respective clear apertures. The direction of measurement is parallel to the original optical axis of the element before the perturbation is applied. TIR is measured in mm. Decentre or roll is measured perpendicular to the optical axis in mm.

Decentred tolerances for two lenses field corrector

Element n°	Front radius	Back Radius	Element wedge Tir	Arcmin	Element Tilt Tir	Arc min	El. Dec/Roll Tir	mm
1	-9509.00000	(MIRROR)			0.0000	0.0	0.0027	0.0100
2	-4374.00000	(MIRROR)			0.0000	0.0	0.0016	0.0080
3	1333.50000	2304.10000	0.0120	0.1	0.0704	0.5	0.0146	0.1000
4	-1295.70000	-10000.00000	0.0100	0.1	0.1132	1.0	0.0264	0.1000
5	INF	INF	0.0500	0.5	0.1097	1.0	0.0000	1.0000
6	2304.10000	1223.20000	0.0300	0.3	0.1078	1.0	0.1413	1.0000

Tab. 2.17 - Decentred tolerances for two lenses field corrector

Decentred tolerances for one lens field corrector and ADC

Element n°	Front radius	Back Radius	Element wedge Tir	Arcmin	Element Tilt Tir	Arc min	El. Dec/Roll Tir	mm
1	-9509.00000	(MIRROR)			0.0000	0.0	0.0027	0.0100
2	-4374.00000	(MIRROR)			0.0000	0.0	0.0016	0.0080
3	2371.40000	INF	0.0120	0.1	0.0420	0.3		
3- 4	2371.40000	INF	0.0588	0.4	0.0193	0.100		
4	INF	INF						
5	INF	INF	0.0200	0.2				
5- 6	INF	10000.00000	0.1284	1.0	0.0044	0.1000		
6	INF	10000.00000						
7	-1223.20000	-10000.00000	0.0200	0.2	0.0391	0.3	0.0282	0.1000
8	INF	INF	0.0500	0.5	0.1095	1.0	0.0000	1.0000
9	2304.10000	1223.20000	0.0300	0.3	0.1078	1.0	0.1415	1.0000

Tab. 2.18 - Decentred tolerances for one lens field corrector and ADC

The values of MTF (Modulation Transfer Function) obtained for the ideal optical system and for the system with tolerances, were computed statistically at the Nyquist frequency of 33 cycles/mm (corresponding to one pixel of 15 μ). The result for the two lenses and ADC and lens corrector were respectively reported in tab. 2-19 and 2-20. The values of MTF obtained considering the tolerances reported in tab. from 2-15 up to tab. 2-18 for each configuration, follow a gaussian distribution. They are reliable with the 97.7% of probability. When the dependence on tolerances is considered, the distance variation between M2 and M1 must be considered as a compensator and it is expressed in mm. Both MTF values with tolerances of the optical system and compensator values for the different fields of view follow a gaussian distribution. They can be considered as mean values with an error range of 2 sigma.

Performance of polychromatic MTF for two lenses field corrector (320 ÷ 1014nm)				
Relative field	Freq L/mm	MTF Design	MTF Design + Tol	Compensator Range (+/-) Displacement S2 (M2)
0.00, 0.00	33.00	0.543	0.496	2.138276
0.00, 0.48	33.00	0.565	0.508	2.138276
0.00, 0.71	33.00	0.479	0.416	2.138276
1.00, 0.71	33.00	0.409	0.330	2.138276
0.00, 1.00	33.00	0.345	0.290	2.138276

Tab. 2.19 - Performance of polychromatic MTF for two lenses field corrector (320 ÷ 1014nm) at z=0

Performance of polychromatic MTF for ADC and one lens corrector (365 ÷ 1014nm)				
Relative field	Freq L/mm	MTF Design	MTF Design + Tol	Compensator Range (+/-) Displacement S2 (M2)
0.00, 0.00	33.00	0.521	0.394	2.135844
0.00, 0.48	33.00	0.606	0.501	2.135844
0.00, 0.71	33.00	0.406	0.351	2.135844
1.00, 0.71	33.00	0.440	0.369	2.135844
0.00, 1.00	33.00	0.312	0.263	2.135844

Tab. 2.20 - Performance of polychromatic MTF for ADC and one lens corrector (365 ÷ 1014nm) at z=0

2.8 FIRST STAGE OF BAFFLES DESIGN

In Fig.2-20 a preliminary baffle design reported, in which the whole field of view is unvignetted, so the diameters of the baffle tubes and central obscuration become quite large. The M1 light loss due to M2 obscuration is of order of 7%, with M1 hole diameter of 600 mm . With the front baffle tube, on M2, the central obscuration is larger and the corresponding M1 light loss becomes of order of 17%.

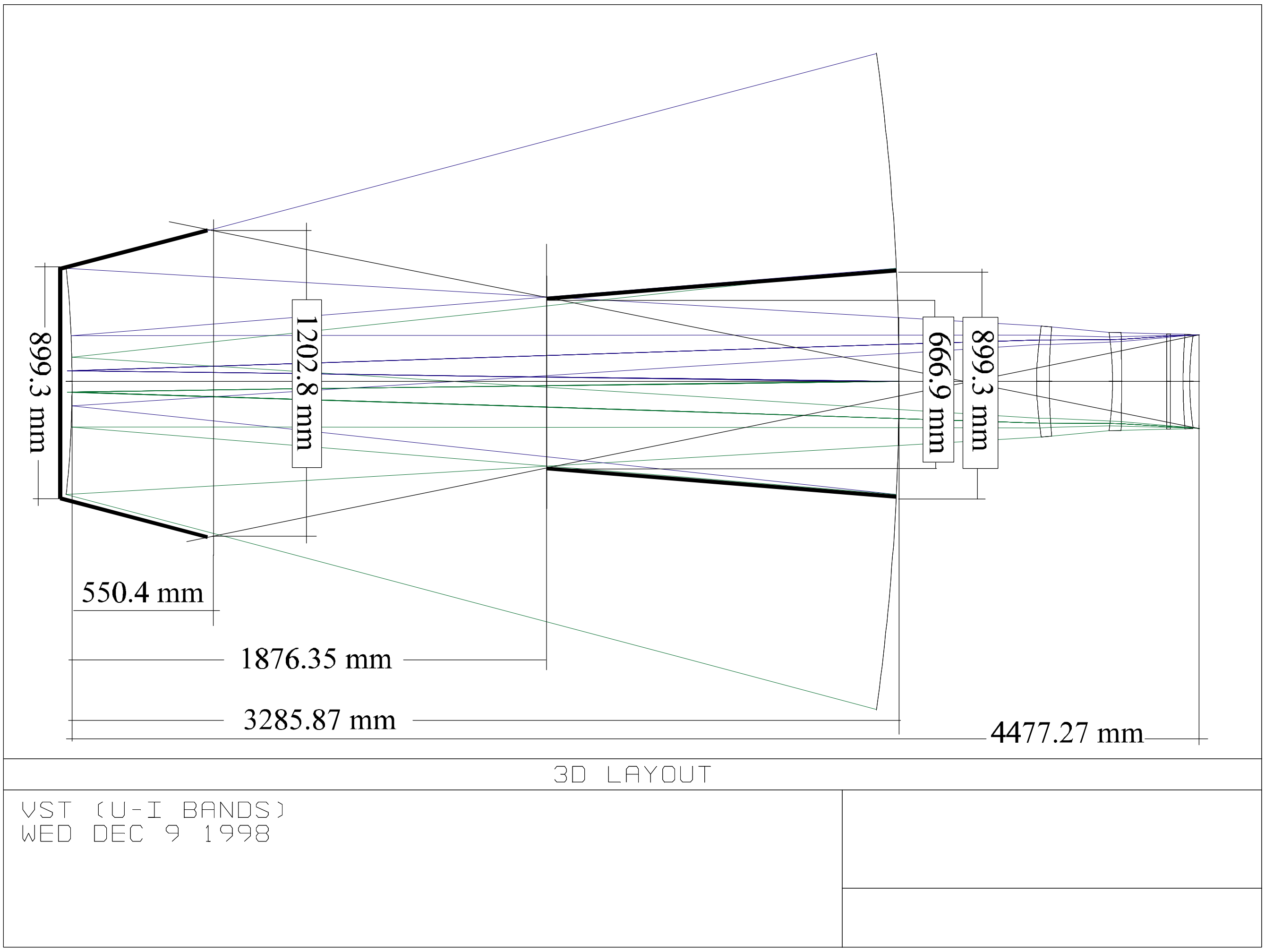

Fig.2.20 - First stage of baffle design

2.9 IMAGE QUALITY VERSUS MIRROR DEFORMATION

In order to evaluate the optical performance of the telescope after the deformations induced on the primary mirror by gravitational loads, mirror optical data were utilized to create the finite element model described in section 4. The model was performed with MSC PATRAN FEA preprocessor tool and analyzed with the MSC Nastran FEA Solutor tool. For the final optical quality analysis it is necessary to have information about both undeformed and deformed mirror interpolated surface with displacements obtained with MSC-NASTRAN FEA. This data set must be passed to Zemax optical analysis tool in a particular file format.
In order to have an automatic and standard interface between the FEA output and Zemax ray tracing tool input, and optimize the real image quality with a control loop, a new procedure was implemented.
The output of the finite element analysis model (FEA) was manipulated with a new dedicated software tool implemented in OAC technological laboratories, and constituted the feedback for the mirror optical surface shape deformation. The global mirror with interpolated surface and its appropriate format were obtained by means of an OAC interface data file creation tool made in C++ and running under Windows 95.
In Fig.2.21 the flowchart of the procedure implemented for the optimization of the system optical quality is shown.

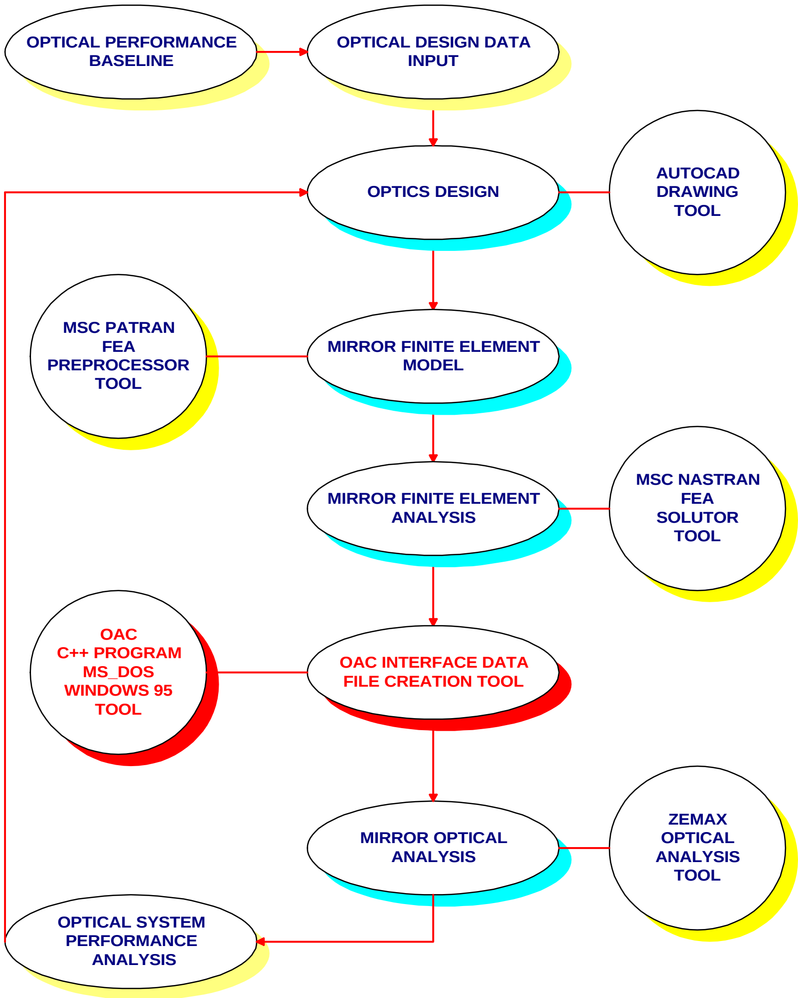

Fig.2.21 - OAC Telescope optical quality optimisation work flow

2.9.1 *Image quality versus mirror deformation for two lenses corrector*

The study of optical quality depreciation due to primary mirror surface deformations for gravitation was performed for both correctors. The analysis has been done with telescope at zenith, that represents the worst case. Fig. 2.22 shows the curves of polychromatic diffraction encircled energy versus centroid distance, for the different fields of view. The radius of the centroid in which the 80% of encircled energy (normalised to diffraction limit) is enclosed is 12.5 µm (1.67pxl), so there is a EE% depreciation of 25% in respect to the design value.
Spot diagrams are shown in Fig.2.23 where the maximum increment of rms spot radius respect to the design value is about of 11%.
Figures 2-24 shows the distance from the best focal plane and the paraxial focal planes of sagittal and tangential rays (field curvature) and distortion curves. The maximum distortion is about 0.013% at the edge of the field for λ =1.014 µm, so it is unchanged in respect to the design value.

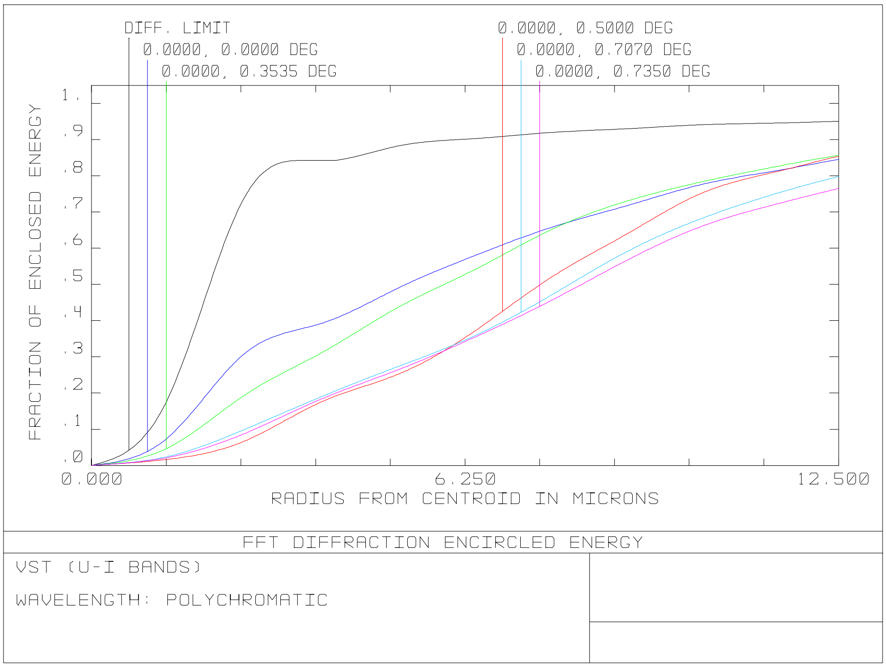

Fig.2.22 - Encircled Energy for two lenses field corrector at zenith with M1 gravitational loads applied

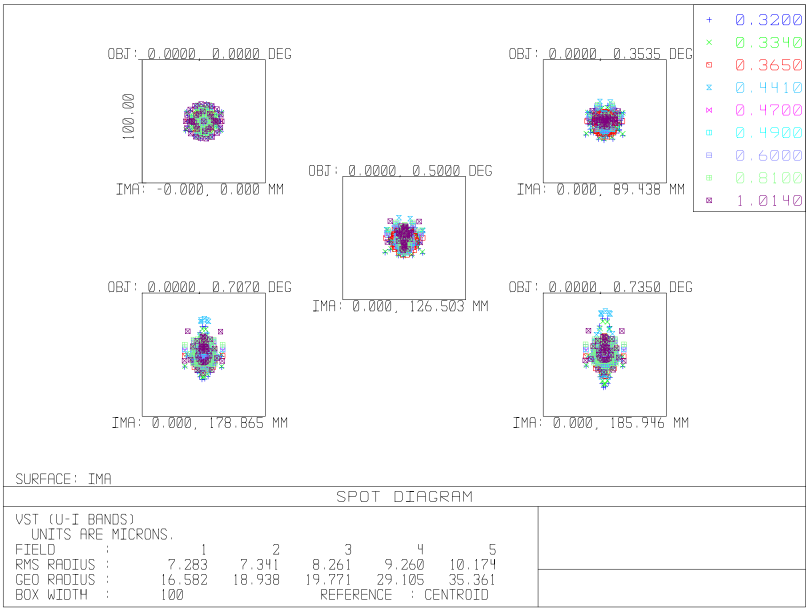

Fig.2.23 - Spot diagram with two lenses corrector at zenith with M1 gravitational loads applied

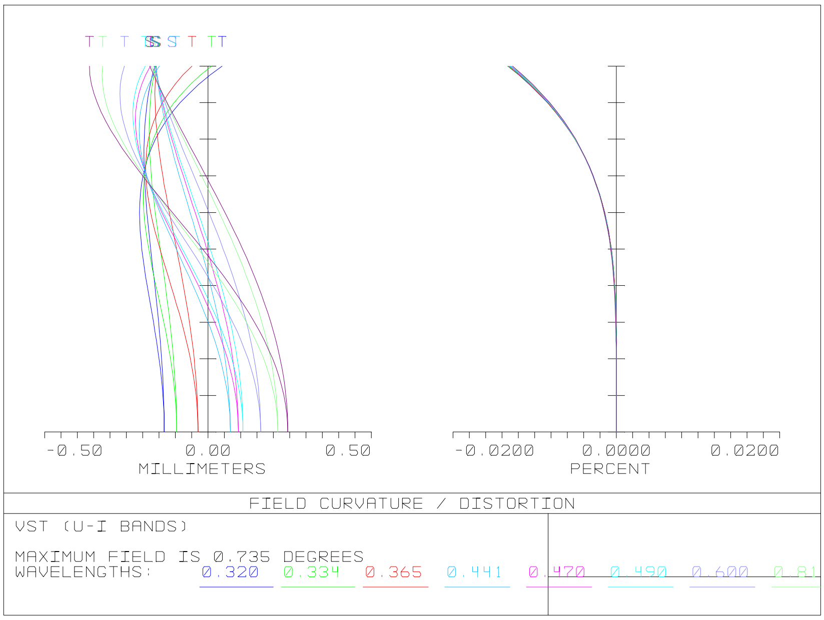

Fig.2.24 - Field curvature and distortion curves for the configuration with two lenses at zenith with M1 gravitational loads applied

2.9.2 Image quality versus mirror deformation for ADC and one lens corrector

In Fig. 2.25 the the curves of polychromatic diffraction encircled energy versus centroid distance, for the different fields of view are reported when gravitational loads are applied to M1 in horizontal position (telescope at zenith). The radius of the circle from centroid in which the 80% of encircled energy (normalised to diffraction limit) is enclosed at 0° zenith angle including primary mirror surface deformations is 11.25 µm (1.5 pxl), so there no deterioration of EE% respect to the design value.
The spot diagrams are shown in Fig.2.26. The maximum increment of rms spot radius respect to the design value is of order of 19%.
In Figures 2-27, the distance from the best focal plane designed for the optical system and the paraxial focal planes of sagittal and tangential rays (field curvature) and distortion curves for the configuration are reported. The maximum distortion is 0.011% at the edge of the field for λ =1.014 µm, so it is comparable with the design value.

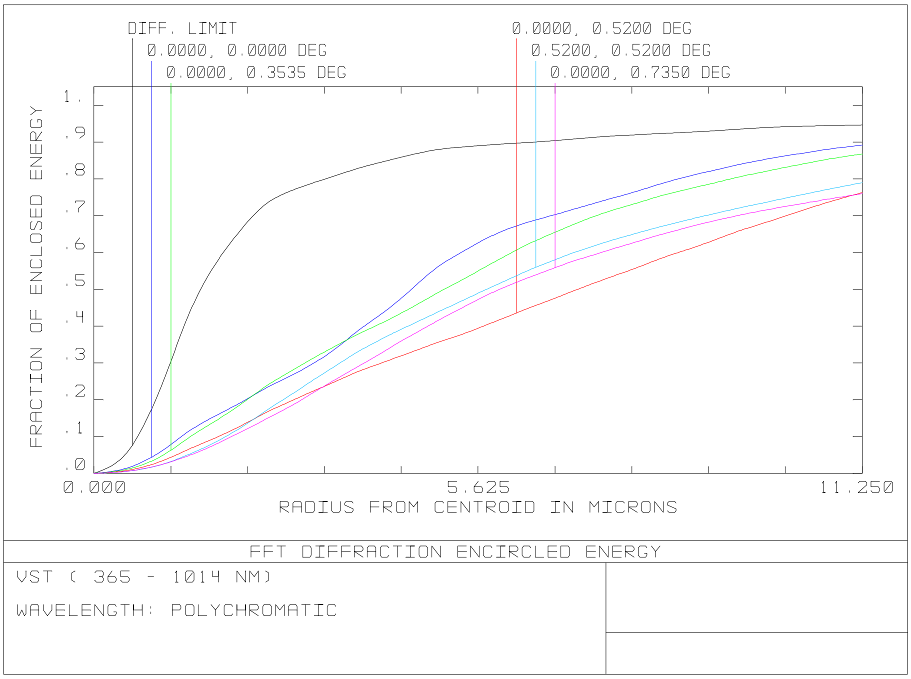

Fig.2.25 - Encircled Energy for two lenses field corrector at zenith with M1 gravitational loads applied

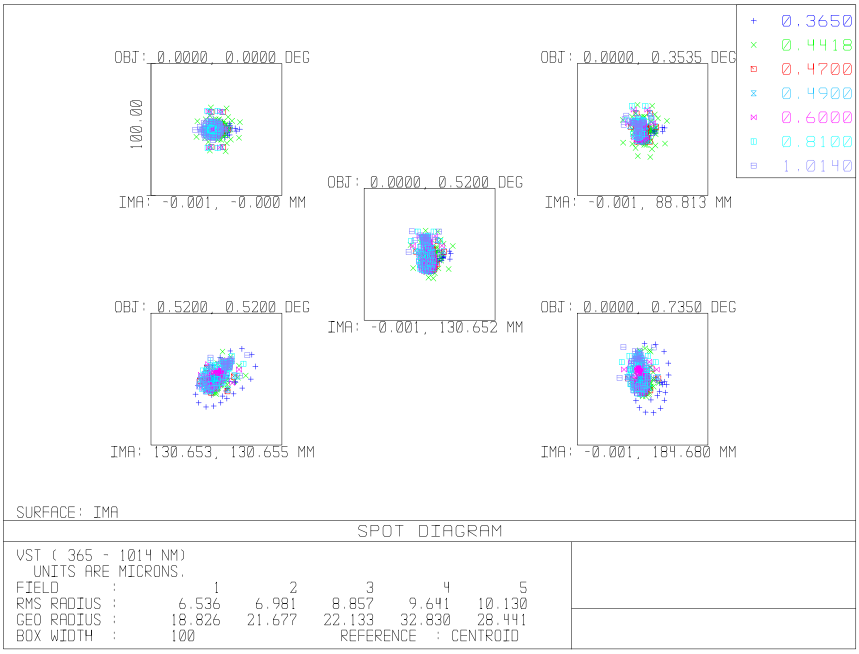

Fig.2.26 - Spot diagram for one lens and ADC at zenith with M1 gravitational loads applied

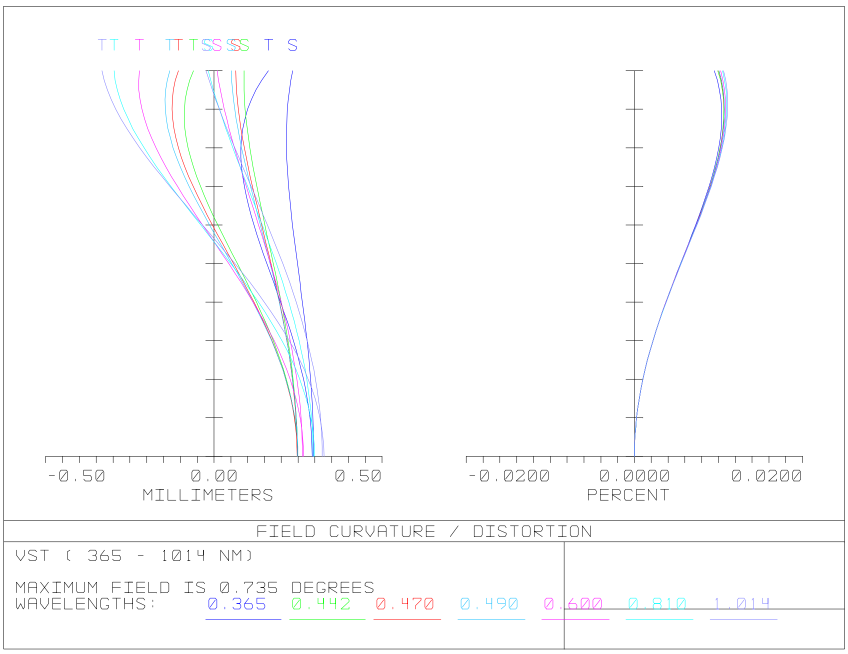

Fig.2.27 - Field curvature and distortion curves for the configuration with one lens and ADC at 0°zenith angle with M1 gravitational loads applied